


ORIGINAL ARTICLE

Special Section: Machine Learning in Agriculture

Unmanned aerial vehicle imagery prediction of sorghum leaf area index under water stress, seeding density, and nitrogen fertilization conditions in the Sahel

Joseph Sékou B. Dembele^{1,2,3}  | Boubacar Gano^{1,3} | Modou Mbaye¹ | Mohamed Doumbia² | Léonce Lamine Dembele² | Mamoutou Kouressy² | Niaba Teme² | Michel Vaksman^{2,4} | Diaga Diouf³ | Alain Audebert⁵

¹Centre d'Etude Régional pour l'Amélioration de l'Adaptation à la Sécheresse (CERAAS), Institute Sénégalais de Recherches Agricoles (ISRA), Route de Khombole, Thies, Senegal

²Institut d'Economie Rurale (IER), LABOSEP de Sotuba, Bamako, Mali

³Laboratoire Campus de Biotechnologies Végétales, Département de de Biologie Végétale, Faculté des Sciences et Techniques, Université Cheikh Anta Diop (UCAD), Dakar-Fann, Dakar, Senegal

⁴CIRAD, UMR AGAP Institut, Montpellier, France

⁵UMR AGAP Institut, Université de Montpellier, CIRAD, INRAE, Institut Agro, Montpellier, France

Correspondence

Joseph Sékou B. Dembele, Centre d'Etude Régional pour l'Amélioration de l'Adaptation à la Sécheresse (CERAAS), Institut Sénégalais de Recherches Agricoles (ISRA), Route de Khombole, Thies, BP 3320, Senegal.
Email: joseph.dembele@yahoo.fr

Assigned to Associate Editor David Clay.

Funding information

CIRAD

Abstract

Sahelian Africa must meet the challenge of providing enough food to meet its growing population. Therefore, novel breeding and intensive production methods are needed to mitigate this challenge. The objective of this study was to calibrate and validate sorghum varieties leaf area index (LAI) values estimated from Unmanned Aerial Vehicle (UAV) at different growing seasons in Senegal and Mali. To achieve this objective, four experiments were conducted with 14 sorghum (*sorghum bicolor*) varieties between 2017 and 2019. At the study sites, LAI was measured and crop reflectance was measured with a multispectral camera mounted on a UAV. The study showed that normalized difference vegetation index (NDVI) and simple ratio (SR) were highly correlated to the area index. The results of validation model revealed a better prediction of measured LAI from NDVI ($R^2 = 0.92$) and SR ($R^2 = 0.89$) vegetation indices in 2019 dry season in Senegal. In addition, the LAI predictions for Mali from NDVI ($p < 0.01$) and SR ($p < 0.01$) were highly correlated. Findings showed that vegetation indices can be used to estimate LAI in Mali and Sahel.

1 | INTRODUCTION

Agricultural production must double to meet the world's food demand, which is expected to exceed 9 billion people before 2050 (Ray et al., 2013). Achieving this goal for sub-Saharan

Abbreviations: LAI, leaf area index; NDVI, normalized difference vegetation index; SR, simple ratio; UAV, unmanned aerial vehicle.

This is an open access article under the terms of the [Creative Commons Attribution-NonCommercial](https://creativecommons.org/licenses/by-nc/4.0/) License, which permits use, distribution and reproduction in any medium, provided the original work is properly cited and is not used for commercial purposes.

© 2024 The Authors. *Agronomy Journal* published by Wiley Periodicals LLC on behalf of American Society of Agronomy.

Africa will be very difficult (McIntyre et al., 2009). In the Sahelian region, low nitrogen availability, lack of resilient improved varieties, adapted seeding density, and agronomic practices are the major factors limiting sorghum (*sorghum bicolor*) production (Gondal et al., 2017; Melaku et al., 2017; Smale et al., 2018). Therefore, to increase the cereal production per unit area, it is necessary to select varieties with high yield potentials under adverse climatic conditions (Chawade et al., 2018, 2019; Leakey et al., 2009). Breeding performant varieties is probably the most effective way to increase crop yields and solve the food security problem in the African-Sahelian region. To speed up the breeding programs, breeders must develop techniques to accurately collect traits of interest to discriminate variation among cultivars (Wezel et al., 2014).

However, many breeding programs rely on laborious manual plant height and leaf area index (LAI) data collection to select cultivars for additional research (Chapman et al., 2014). New phenotyping methods offer a non-destructive rapid imagery-based phenotyping approach at low cost (Gracia-Romero et al., 2017; Yang et al., 2017). These technologies provided high-quality images to predict growth traits and cereal yields under various growing conditions (water stress, mineral fertilization, and seeding density) (Fiorani & Schurr, 2013; Gracia-Romero et al., 2018; Shafian et al., 2018). The LAI is defined as the total leaf area per unit ground area. It provides information that is crucial for understanding photosynthesis, evapotranspiration, primary production, mass, and energy exchanges at different scales (Soudani et al., 2001). The LAI is a key variable that is strongly associated with crop canopy, crop growth, light energy interception, and grain yield (Huang et al., 2016; Towers et al., 2019). According to Jin et al. (2013), LAI is a phenotypic trait that best explains crop yield (grain and straw) and is functionally related to the spectral reflectance of the crop canopy. Previous work demonstrated that remote sensing can be used to predict LAI in maize (*Zea mays* L.) and wheat (*Triticum aestivum* L.), but little research has been done on sorghum (Potgieter et al., 2017). Therefore, this paper fills this gap, thus aimed to calibrate and validate the LAI at different cropping seasons using unmanned aerial vehicle (UAV)-based vegetation indices in the Sahel. Specifically, we determined the relationships between UAV-based normalized difference vegetation indices (NDVI) and simple ratio (SR) with LAI for sorghum cultivars under water stress, nitrogen fertilization, and seeding density. We also studied the cultivars response under nitrogen fertilization and seeding density.

2 | MATERIALS AND METHODS

2.1 | Study sites

Two calibration trials were conducted in the 2017 rainy and 2018 dry seasons (Figure 1A) at Bambey, Centre National de Recherche Agronomique (CNRA) (14°42'N; 16°28'W),

Core Ideas

- Normalized difference vegetation index and simple ratio were highly correlated to the leaf area index.
- Leaf area index was predicted from normalized difference vegetation index and simple ratio.
- Diversity among varieties was studied from normalized difference vegetation index and simple ratio.

Senegal. Bambey climate is of the Sudano-Sahelian type, characterized by a long dry season from November to June and a short rainy season from July to October. The monthly average temperature and cumulative annual rainfall in 2017 were 30°C and 436.7 mm respectively. In 2018, the monthly average temperature recorded during the dry season was 28°C. Experiments in 2017 rainy and 2018 dry seasons were conducted on sandy loam soils (97.7%) with a high sand content (Gano et al., 2021). For model validation, two experiments were conducted in 2019 dry season at the CNRA of Bambey in Senegal and 2018 rainy season at Station de Recherche Agronomique de Sotuba (SRAS) in Mali (12°39' N; 07°56' W) (Figure 1B). The 2019 trial in Bambey was conducted on a sandy-silty soil type (95.7%) with an average monthly temperature of 29°C. The climate of Sotuba is the Sudano-Sahelian type with a rainy season from May to October according to the crop zones. Sotuba's cumulative annual rainfall and monthly average temperature recorded in 2018 were 840 mm and 27°C respectively. Trial was conducted on a sandy-silty soil type (96.84%) with a low clay content of 3.85% (Dembélé et al., 2020).

2.2 | Plant materials

In Bambey, 10 contrasted sorghum varieties for different agro-morpho-physiological traits were used in 2017 rainy and 2018 dry seasons for model calibration. Varieties include three hybrids (FADDA, PABLO, and NIELENI) and seven open-pollinated improved cultivars (SOUMBA, GRINKAN, SOUMALEMBA, JAKUMBE, SAMSORG17, FAOUROU, and F20-20) (CEDEAO-UEMOA-CILSS, 2016; Gano et al., 2021). These varieties originated from Mali, Nigeria, and Senegal and represent the diversity of sorghum grown in West Africa. For model validation, 10 sorghum varieties were conducted in 2019 dry season in Bambey, Senegal, under different water regimes (irrigated and stressed) for model calibration. To test model validations in another environment, data were collected in 2018 rainy season at Sotuba, Mali, under two different seeding densities (26,600 plants ha⁻¹ and 53,300 plants ha⁻¹) and three nitrogen fertilization doses (0 kg ha⁻¹,

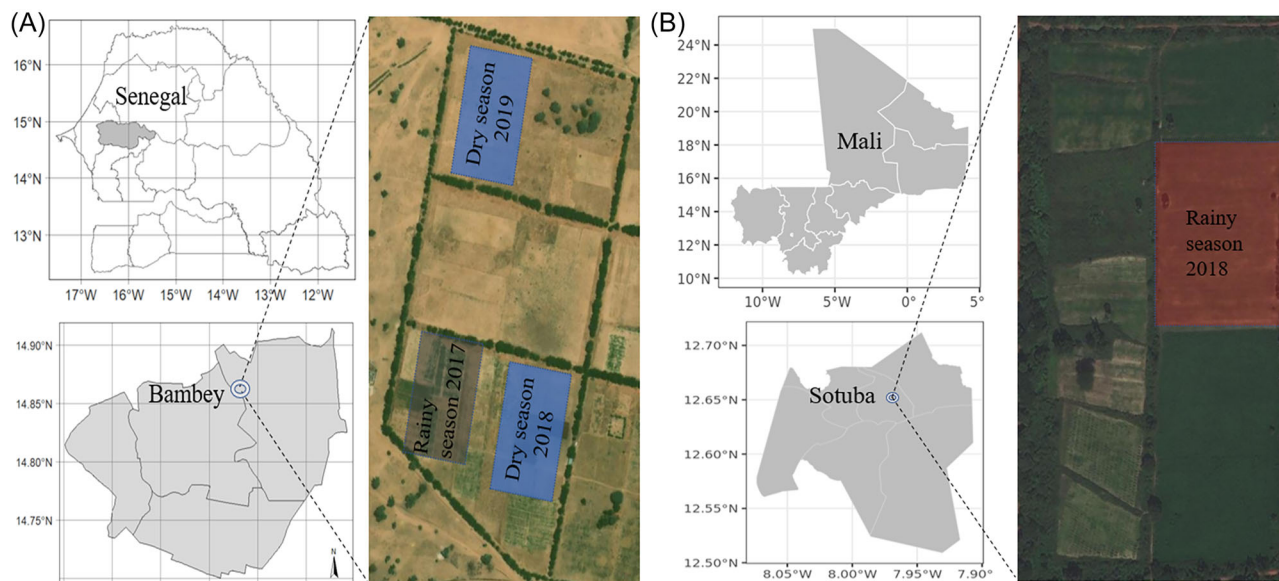


FIGURE 1 Sites of the experiments. (A) Bambeý (Senegal) in 2017 rainy and 2018 and 2019 dry seasons; (B) Sotuba (Mali) in 2018 rainy season.

89 kg ha⁻¹, and 178 kg ha⁻¹) on eight reference sorghum varieties for intensification, were used. Hybrid varieties used were (FADDA and PABLO), open-pollinated varieties (SOUMBA, GRINKAN, C2_007-03, C2_075-15, and A12-79) and the local variety (TIEBILE) (Dembélé et al., 2021). Varieties used across Bambeý and Sotuba were FADDA, PABLO, SOUMBA, and GRINKAN.

2.3 | Experimental designs and trial managements

2.3.1 | Calibration trials

The experimental design used at Bambeý in 2017 rainy season was a split-plot with nitrogen as main factor at three levels (0 kg ha⁻¹, 100 kg ha⁻¹, and 200 kg ha⁻¹) and 10 sorghum varieties replicated thrice. Sowing distances were 0.60 m between rows and 0.30 m between hills on the row. Each plot was 4.5-m long and 6.60-m wide. Thinning was performed 15 days after sowing to one plant per hill. Basal application of 150 kg ha⁻¹ granulated triple superphosphate (0–45–0) was applied prior to sowing. Urea (46–0–0) was applied in two splits, after thinning (50%) and before panicle initiation (50%). In 2018 Bambeý dry season trial, a split-plot design with three replicates was used. There were two factors, including water regime (irrigated and stressed) as main factor and 10 sorghum varieties used in 2017. For non-stressed plots, about 50 mm (2 by 25 mm) of plot was supplied per week until physiological maturity. In stressed plots, the irrigation was withheld 30 days after sowing at vegetative stage for 3 weeks. For mineral fertilization, 150 kg ha⁻¹ of NPK (17–17–17) was applied homogeneously after sowing and 50 kg

ha⁻¹urea (46–0–0) was applied at panicle initiation period. Two manual weedings were carried out in each experiment.

2.3.2 | Validation trials

The 2019 dry season trial was a repeat of the 2018 dry season study in Bambeý, Senegal. The 2018 rainy season trial in Sotuba, Mali, was conducted following a split-split-plot design with three factors and three replicates. Two seeding densities (26,600 plants ha⁻¹ and 53,300 plants ha⁻¹) and three nitrogen levels (0, 89, and 178 kg ha⁻¹) were applied on eight sorghum varieties in Mali. Sowing distances were 0.75 m between rows and 0.25 m (high) and 0.50 m (low) density between hills on the row. Experimental unit was 18 m² with six rows length of 4.5-m long and 4-m wide each. The experimental soil was plowed to approximately 30-cm depth. The sowing was done on June 18, 2018 and July 5, 2019 after a rainfall of about 30 mm at a rate of five to six seeds per hill (i.e., 8–10 kg of seed ha⁻¹). Thinning was performed 15 days after sowing to one plant per hill (density: 26,600 plants ha⁻¹ and density: 53,300 plants ha⁻¹). Urea (46–0–0) was applied 3 weeks after thinning (50%) and before panicle initiation (50%). Basal application of 146 kg ha⁻¹ of phosphate naturel de Tilemsi (PNT) (0–31–0) granulated was homogeneously made in all plots before sowing. Two manual weedings were conducted in each experiment.

2.4 | Field data collection

LAI measurements were conducted at late flowering (two sampling dates) in 2017 and 2018 in Senegal. For model

TABLE 1 Periods of image acquisition by drone during the different experiments in Senegal and Mali.

Trials	Stages	Days after flight	No. of plots
Rainy season 2017 (Senegal)	Vegetative	35	90
	Vegetative	49	90
	Flowering	63	90
	Flowering end	77	90
	Maturity	91	90
Dry season 2018 (Senegal)	Vegetative	40	60
	Vegetative	47	60
	Flowering	61	60
	Flowering end	75	60
	Maturity	89	60
Dry season 2019 (Senegal)	Flowering	89	60
Rainy season 2018 (Mali)	Maturity	100	144



FIGURE 2 Drone (A), red, green, and blue (RGB) (B), and multispectral (C) cameras used in the image capture during the experiments in Senegal and Mali.

validation, LAI measurement was performed during flowering in the 2019 dry season at Senegal and maturity during the 2018 rainy season in Mali. LAI was measured with a Sunscan Septometer (Delta-T Device Ltd.) following the method of Wilhelm et al. (2000). All field LAI measurements were immediately following the UAV flights (Table 1).

2.5 | UAV data acquisition

Five UAV flights were conducted between crop emergence and flowering in 2017, 2018, and 2019 in Senegal and Mali (Table 1). The UAV (Figure 2A) was a hexacopter (FeHexacopterV2, Mikrokopter) equipped with two cameras, red,

green, blue (RGB) (Figure 2B) and multispectral (Figure 2C), which were consecutively fixed on board at each flight. The visible camera used was an RGB ILCE-6000 digital camera (Sony Corporation) with a resolution of 24.3-megapixel (6000×4000 pixels), equipped with a 60-mm focal length lens. To minimize the blurring effect and noise in the images, the camera was set on speed priority ($1/1250$ s) and auto ISO mode. The images taken were recorded in JPEG format on a secure digital (SD) memory card. The second camera was a multispectral camera (www.hiphen-plant.com) equipped with an 8-mm focal length lens and an integrated GNSS system. The multispectral camera acquires 1280×960 -pixel images at six independent spectral bands (450, 530, 560, 675, 730, and 850 nm) with a spectral resolution of 10 nm. Images were stored in a Tag Image File Format (TIFF) format. The Kopter Tools application software was used to automatically design the flight plan and schedule the image capture to cover the entire trial area and ensure an 80% overlap between images. To reduce the effects of ambient light conditions, we limited flight to clear and cloudless days between 10:00 and 12:00 a.m. (Greenwich Mean Time) allowing plants shadow effect reduction. Flight was made at an altitude of 25 m above ground level with a speed of 4.5 m s^{-1} . In this configuration, we obtained a ground resolution of around $0.6 \text{ cm pixel}^{-1}$ for RGB camera and $2.7 \text{ cm pixel}^{-1}$ for multispectral camera. To obtain accurate reflectance values during image processing, a radiometric calibration target, a carpet panel of (2.5 m^2) was placed horizontally on the ground 2 m from the sorghum plants to limit proximity effects. Nine gray coloreds ground control points (GCPs) were uniformly distributed at different angles of the field area with fixed position for all flights throughout the experiment and were surveyed using Precis BX305 Real Time Kinematics (RTK) GNSS unit (Terminus GNSS Inc.) (Gano et al., 2021; Jay et al., 2019; Roupsard et al., 2020).

2.6 | Image processing and extraction of vegetation indices

After UAV flights, the images were concatenated to generate a geo-referenced ortho-image multilayer using Agisoft PhotoScan (PhotoScan Professional 1.4; Agisoft LLC). Radiometric calibration and geometric correction of the ortho-image were done with the Agisoft PhotoScan software according to Rouspard et al. (2020). The delimitation of plots on geo-referenced ortho-image were conducted using geographic information software QGIS (version 3.2), which allowed the generation of a shapefile with geographical information of the different plots. The extraction of each vegetation index average values for each elementary plot was conducted using the R software (packages, Raster, sf). Plant indices computed for this study were the NDVI and SR following the formulas of Equations (1) and (2). Generated data were stored in CSV format for comparison with field data (Rouse et al., 1973; Gitelson & Merzlyak, 1998).

$$\text{NDVI} = \frac{\rho\text{NIR} - \rho\text{R}}{\rho\text{PIR} + \rho\text{R}} \quad (1)$$

$$\text{SR} = \rho\text{NIR}/\rho\text{R} \quad (2)$$

2.7 | Statistical analysis

Statistical analyses were performed using software R, version 3.6.2 in environment (Venables et al., 2016). Regression models were developed to calibrate and validate the LAI using NDVI and SR vegetation indices calculated from UAV images. The calibration involved data from 690 plots collected in 2017 rainy and 2018 dry seasons in Senegal (field and UAV data). A first model validation was performed on LAI data from 60 plots collected at flowering in the 2019 dry season in Senegal. The second validation of the model involved LAI data from 120 plots collected at maturity in the 2018 rainy season in Mali. Coefficient of Determination (R^2) and root mean square error (RMSE) were calculated to assess the performance of regression models. The R^2 and RMSE were determined using the following equations:

$$R^2 = 1 - \frac{\sum_{i=1}^n (y - \hat{y})^2}{\sum_{i=1}^n (y - \bar{y})^2} \quad (3)$$

$$\text{RMSE} = \sqrt{\sum_{i=1}^n \frac{(y - \hat{y})^2}{n}} \quad (4)$$

where n is the number of observations; i is the i th measured value; y is the measured value; \hat{y} is the estimated value by UAV; and \bar{y} is the average of measured value.

Measured LAI and predicted LAI data calculated from NDVI and SR in 2018 rainy season were subjected to analysis of variance (ANOVA) using the split-split-plot model developed by Carmer et al. (1989). Treatments means were separated using least significant difference (LSD) at the 5% threshold of probability.

3 | RESULTS

3.1 | Model calibration

For model's calibration purpose, we used data collected in Senegal in 2017 rainy and 2018 dry seasons to depict the temporal evolution of plant LAI trait and UAV derived indices to seek for relationships.

3.1.1 | Growth dynamics of LAI, NDVI, and SR

LAI values increased gradually from first to fifth measurement in 2017 rainy and 2018 dry, seasons in Senegal (Figure 3). Maximum LAI values were reached at flowering in 2017 (77 days after sowing [DAS]) and 2018 (75 days after sowing, DAS) and decreased with leaf senescence in early maturity (91 DAS in 2017 and 89 DAS in 2018). This reduction was more pronounced in 2017 rainy season compared to 2018 dry season (Figure 3). Overall, LAI value was higher in dry season than in the rainy season. The NDVI and SR vegetation indices in 2017 rainy season and 2018 dry season showed identical growth dynamics trends to those of LAI evolution measured at different UAV flight dates. The peak for NDVI and SR was obtained at the end of flowering in both years experiments, but with slightly decreased in dry season. However, a significant drop in NDVI and SR was observed in rainy season (Figure 3). This result shows that NDVI and SR vegetation indices evolution follows measured LAI progression.

3.1.2 | Relationship between vegetation indices and LAI

A linear regression model was performed to establish relationships between vegetation indices and measured LAI (Figure 4). The regression models used were significant at the 1% threshold (Table 2). The NDVI showed a strong relationship ($R^2 = 0.72$) with the measured LAI (Figure 4A) and

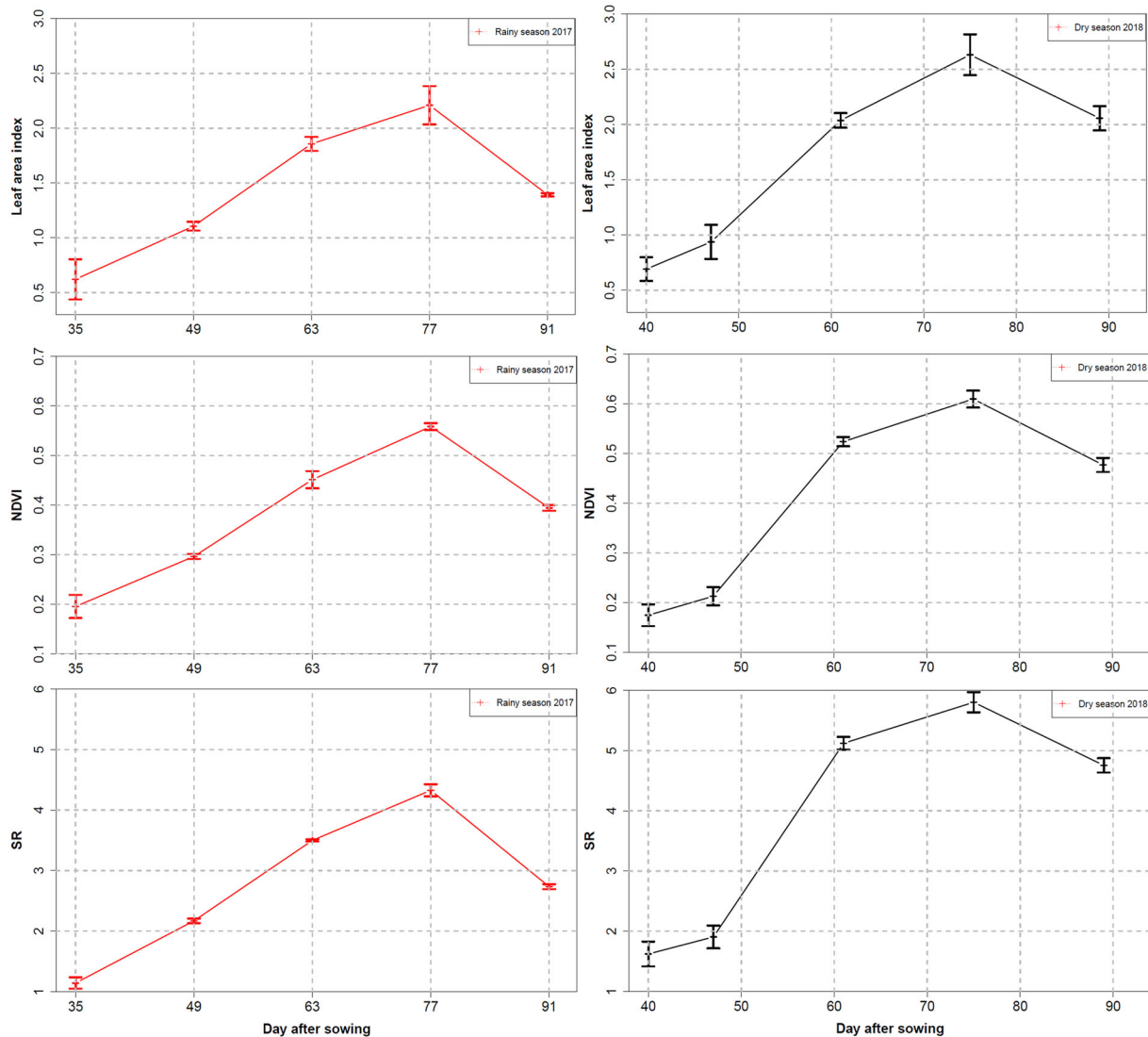


FIGURE 3 Evolution of leaf area index (LAI), normalized difference vegetation index (NDVI), and simple ratio (SR) at different measurement dates (field and drone flight) in 2017 rainy and 2018 dry seasons in Bambey, Senegal.

TABLE 2 Regression models developed between normalized difference vegetation indices (NDVI), simple ratio (SR), and leaf area index (LAI) measured in 2019 dry season in Senegal and 2018 rainy season in Mali.

Test	Vegetation indices	Sample numbers (<i>n</i>)	Traits	Regression models	R^2	RMSE	<i>p</i> -value
Calibration	NDVI	690	LAI	$y = 8.697x^2 - 3.026x + 0.793$	0.72	0.3	<0.001
	SR	690		$y = -0.009 \times 2 + 0.532x - 0.185$	0.74	0.28	<0.001
Validation 2019	NDVI	60		$y = 0.825x + 0.149$	0.92	0.31	<0.001
	SR	60		$y = 0.858x + 0.219$	0.89	0.37	<0.001
Validation 2018	NDVI	120		$y = 0.535x + 1.316$	0.61	0.4	<0.01
	SR	120		$y = 0.402x + 1.685$	0.58	0.45	<0.01

RMSE value was 0.30 (Table 2). The NDVI values ranged from 0.06 to 0.82. The SR was correlated to measured LAI with an R^2 of 0.74 (Figure 2C) and a RMSE of 0.28 (Table 2). These values ranged from 1.03 to 11.15 (Figure 4C). LAI val-

ues ranged from 0.07 to 5.7 among varieties, developmental stages and years, respectively. The calibration model gave a better regression between calculated LAI and measured LAI (Figure 4B,D).

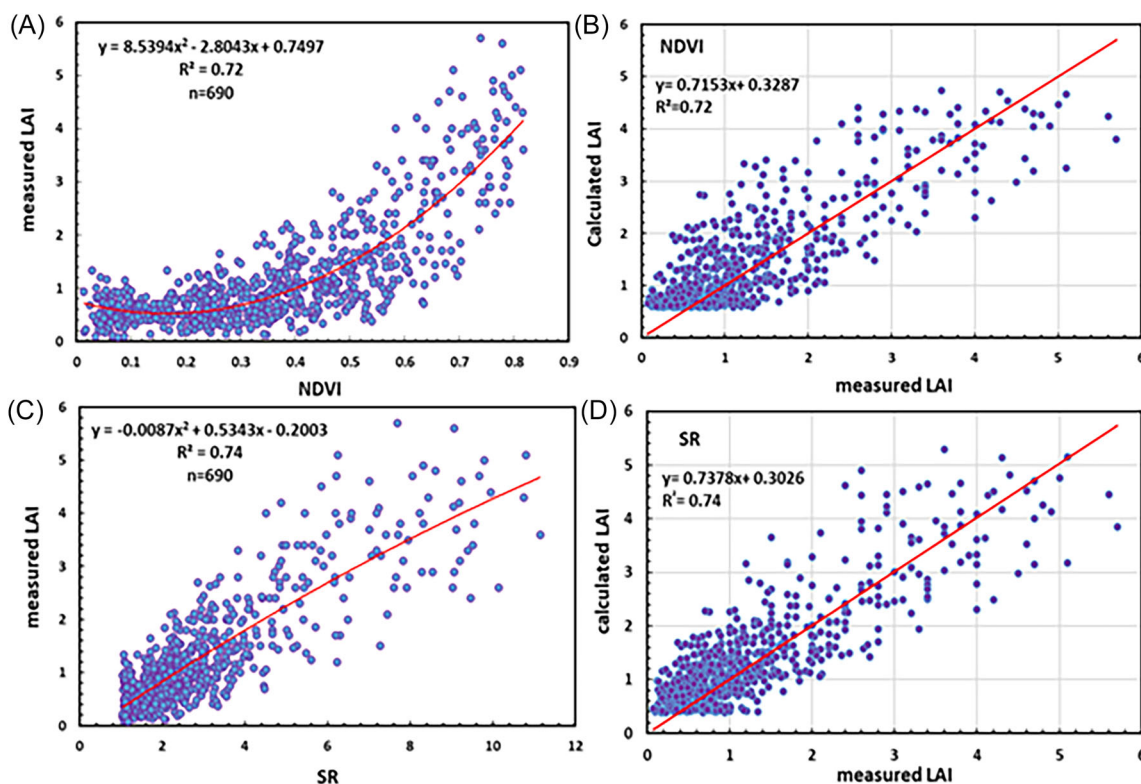


FIGURE 4 Calibration models between measured leaf area index (LAI), normalized difference vegetation indices (NDVI), and simple ratio (SR) (A and C); and between measured LAI and calculated LAI (B and D) in 2017 rainy and 2018 dry seasons in Bambey, Senegal. R^2 , coefficient of determination.

3.2 | Models' validation

Data collected during the 2018 Mali rainy season and 2019 Senegal dry season were used for validation.

3.2.1 | Prediction of the LAI from vegetation indices

Figure 5 showed linear regression between predicted LAI and measured LAI at Bambey (Senegal) and Sotuba (Mali). The R^2 for model validation was calculated and the ability of vegetation indices to predict measured LAI was identified by the RMSE. The relationship between measured LAI and NDVI and SR in Senegal was highly significant ($p < 0.001$, $R^2 = 0.92$, $RMSE = 0.31$) for NDVI and ($p < 0.001$, $R^2 = 0.89$, and $RMSE = 0.37$) for SR (Figure 5A,B; Table 2). In addition, the prediction accuracy between predicted LAI and measured LAI at Sotuba in Mali was acceptable for NDVI ($p < 0.01$, $R^2 = 0.61$, and $RMSE = 0.40$) and SR ($p < 0.01$, $R^2 = 0.58$, and $RMSE = 0.45$) (Figure 5C,D; Table 2). Prediction models performed less in Mali due to overestimation and under-estimation of the models at the beginning of the vegetative and maturity stages respectively (Figure 5C,D).

3.3 | Variation in seeding density, nitrogen, and varieties based on LAI and vegetation indices in 2018 rainy season in Mali

ANOVA of data from the model validation under seeding density and nitrogen fertilization was performed. It was based on 2018 rainy season data collected from 120 plots at Sotuba. Results showed a significant variety effect on measured LAI and calculated LAI from NDVI (LAI_NDVI) and SR (LAI_SR) ($p < 0.001$). However, no significant difference was observed between seeding density and nitrogen on measured LAI, LAI_NDVI, and LAI_SR (Table 3). FADDA, A12-79, C2_075-15, C2_007-03, and GRINKAN varieties recorded the highest measured LAI values with an average of 3.2. PABLO and SOUMBA varieties were the least performing for measured LAI. C2_075-15, FADDA, C2_007-03, A12-79, and GRINKAN varieties performance was constant for LAI_NDVI with an average value of 3.06, and PABLO and SOUMBA varieties were the least performing for LAI_NDVI. The C2_075-15, C2_007-03, FADDA, GRINKAN, A12-79, and TIEBILE varieties produced highest LAI_SR values with an average value of 2.77. PABLO and SOUMBA varieties were the least performing for LAI_SR values (Table 3).

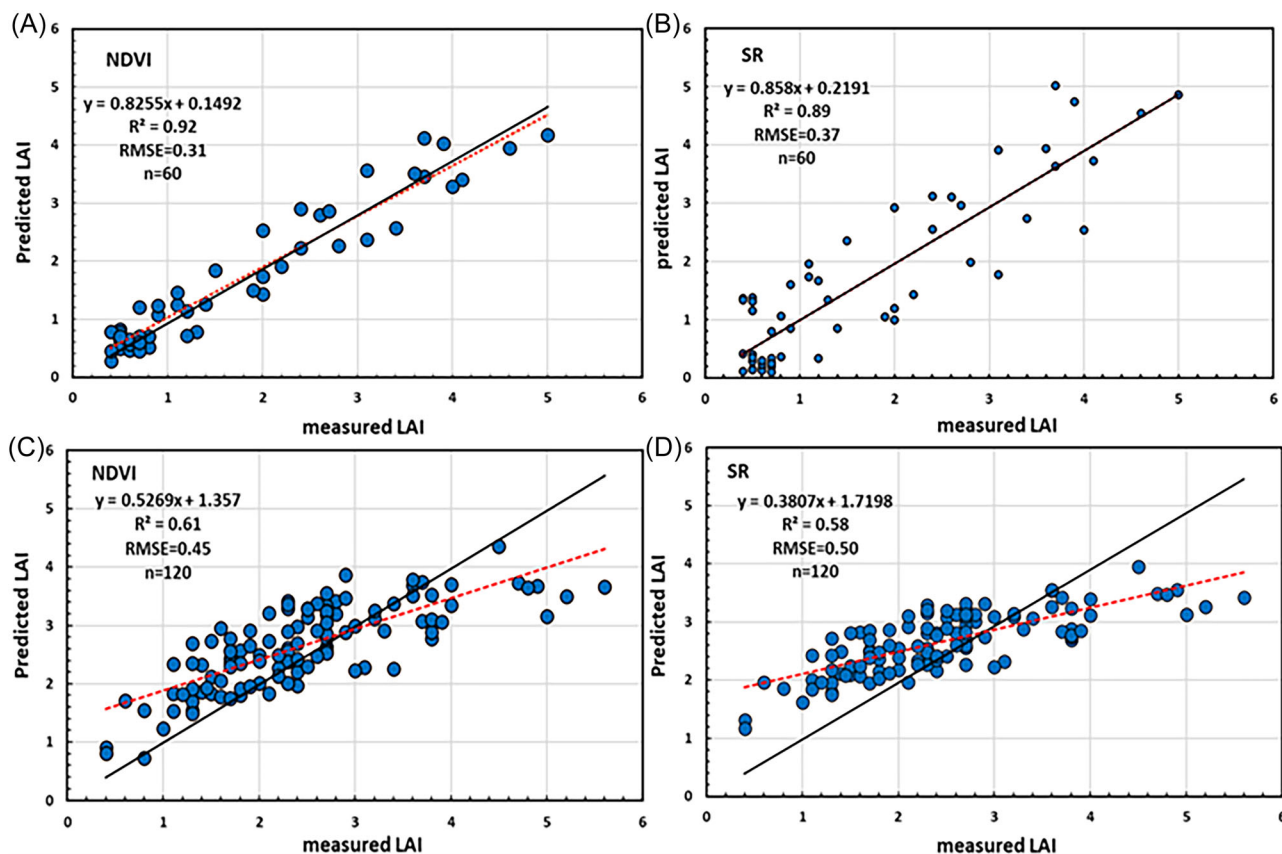


FIGURE 5 Validation test: Relationship between measured leaf area index (LAI) and LAI calculated from normalized difference vegetation index (NDVI) and simple ratio (SR) in 2019 dry season in Bambe, Senegal (A and B) and 2018 rainy season in Sotuba, Mali (C and D). RMSE, root mean square error.

4 | DISCUSSION

This study established relationships between LAI and NDVI and SR derived from UAV imagery in the 2017 and 2018 wet and dry Senegal seasons, respectively. The calibrated models provided a good LAI prediction during the 2018 and 2019 wet and dry seasons, respectively, in Mali and Senegal, and varieties effects on LAI under nitrogen fertilization and seeding density in 2018 in Mali.

4.1 | Plant growth dynamics determination under different conditions with UAV imagery

Results showed that NDVI and SR vegetation indices were highly correlated to LAI in the 2017 rainy and 2018 dry seasons at Senegal (Figure 3). In addition, the measured LAI and NDVI and SR vegetation indices reached their maximum values at flowering and then decreased as the plant matured (Figure 3). NDVI and SR values decrease after flowering was attributed to leaf senescence (Sultana et al., 2014). Numerous research studies have concluded that leaf senescence would cause a reduction in NDVI due to increased red

band reflectance and decreased near-infrared band reflectance (Naser et al., 2020). Leaf senescence was observed in other previous studies conducted under water stress and under low nitrogen application (Raun et al., 2001). Serrano et al. (2000) and Prasad et al. (2007) showed that, in addition to NDVI, SR could be used to detect LAI variation between growing seasons. Our results showed that the LAI and NDVI and SR values were higher in the 2018 dry season than the 2017 rainy season (Figure 3). According to Kouressy et al. (2020), late sowing of photoperiod-sensitive sorghum varieties during the rainy season causes cycle shortening with low dry matter accumulation resulting in a high reduction in straw biomass and LAI. This could help explain why LAI was low during the Bambe 2017 rainy season. Bamba et al. (2019) found similar results in millet (*Pennisetum glaucum*).

4.2 | Models' calibration establishment of sorghum LAI under different conditions

The current study results provide new insight regarding the capacity to estimate LAI of sorghum plants grown under water and N stress. Study results showed the ability of NDVI and

TABLE 3 Analysis of variance of the factors studied on the measured leaf area index (LAI) and LAI calculated from the normalized difference vegetation indices (NDVI), and simple ratio (SR) in 2018 rainy season in Sotuba, Mali.

Treatments	LAI	LAI_NDVI	LAI_SR
Density (D) (plants ha⁻¹)			
26,666 (D1)	2.13a	2.41a	2.47a
53,333 (D2)	2.8a	2.91a	2.82a
Nitrogen (N) (kg N ha⁻¹)			
N0	2.26a	2.52a	2.52a
89 (N1)	2.3a	2.56a	2.62a
178 (N2)	2.83a	2.91a	2.8a
Variety (V)			
FADDA	3.21a	3.03a	2.84ab
C2_075-15	2.8ab	3.06a	2.93a
C2_007-03	2.7ab	2.93ab	2.88a
GRINKAN	2.65b	2.88ab	2.72ab
A12-79	2.96ab	2.71bc	2.67ab
TIEBILE	2.18c	2.41c	2.56b
PABLO	1.87d	2.27d	2.36c
SOUMBA	1.83d	2.25d	2.34c
Source of variation			
V	***	***	***
N	ns [†]	ns	ns
D	ns	ns	ns
V × D	ns	ns	ns
V × N	ns	ns	ns
N × D	ns	ns	ns
V × D × N	ns	ns	ns

Note: Values in a column followed by different letters are significantly different at $P < .05$. Lower-case and upper-case letters indicate comparisons within treatments of each density, nitrogen and among varieties, respectively.

***Significant at the 0.001 probability level. [†]ns, not significant.

SR to predict LAI with high accuracy (Figure 4). Hassan et al. (2018) stated that vegetation indices would be the best option for estimating crop growth parameters in contrasting environments. Our results showed that the Senegal calibration models overestimated LAI before flowering. However, measured LAI was underestimated by the calibration models at the end of flowering (Figure 4B,D). Malambo et al. (2018) attributed this to the time lags between the UAV-based measurements and the field-based measurements. Other researches have shown that overestimation and underestimation of the model may be related to low reflectance in red band before flowering and near infrared band after flowering (Din et al., 2017; Gong et al., 2021). Cheng et al. (2020) and Peng et al. (2011) reported that leaf saturation and senescence at the end of crop cycles are the main causes of model overestimations and underestimations.

4.3 | Models' prediction under different conditions in Senegal and Mali

Our results showed that NDVI and SR predictions were more accurate under water stress in the 2019 dry season than the N stress and seeding density in the 2018 rainy season at Mali. This finding indicates that environmental factors influenced the feasibility of using these models. However, the moderate R^2 values obtained demonstrated that this method can still be deployed in canopy phenotyping of sorghum (Gano et al., 2021). According to Hassan et al. (2018), a moderate R^2 values may be due to limited number of manually measured plants. Thus, the calibration carried out in the 2017 rainy and 2018 dry seasons in Bambey, Senegal, was not representative of the 2018 Mali climatic conditions and cropping practices. It would be interesting to conduct a new calibration to determine whether this overestimation of models is attributed to pedoclimatic conditions or to agronomic practices in Mali. To ensure that these spectral indices can be used as a tool in predicting LAI (Kang et al., 2016) in Mali, a new model may be needed. The methods presented here represent important advances in the non-destructive measurement of the sorghum LAI and can help accurately predict crop growth at flowering and early maturity.

4.4 | Genotypic variation under seeding density and nitrogen fertilization

The development of an approach based on multispectral imagery to evaluate growth parameters of sorghum varieties under seeding density and nitrogen fertilization is an important step for the improvement of crop breeding methods. Results of the ANOVA performed on the 2018 data in Mali (Table 3) showed variability among varieties for measured LAI and predicted LAI. The FADDA, C2_075-15, C2_007-03, and A12-79 varieties recorded the same values for measured and predicted LAI. In contrast, the PABLO and SOUMBA varieties had low measured and predicted LAI values. This suggests that vegetation indices derived from UAV-based imaging can be used in the study of variety variability under nitrogen fertilization and seeding density. This result is similar to that of Yang et al. (2020) who reported variability between wheat varieties for vegetation indices from UAV-based imagery under water stress and nitrogen fertilization.

5 | CONCLUSION

Findings showed that the NDVI and SR vegetation indices could be used to predict LAI growth. Prediction of measured LAI from NDVI ($R^2 = 0.92$) and SR ($R^2 = 0.89$)

vegetation indices was better in the dry season in Senegal. In addition, the prediction of measured LAI from NDVI and SR was of $R^2 = 0.61$ and $R^2 = 0.58$, respectively, at maturity under nitrogen fertilization and seeding density in the rainy season in Mali. This approach based on vegetation indices (UAV imagery) was effective in studying morphological differences among varieties for predicted LAI at early maturity stage in 2018 rainy season in Mali. It suggested a possible use of UAV-based multispectral imaging in sorghum varieties diverse behavior under nitrogen fertilization and seeding density at early maturity in Sotuba, Mali. The results showed that the UAV phenotyping method can be used in sorghum breeding programs in the Sahel especially in Mali to accelerate selection of new cultivars and increase efficiency of work. Further work should be done to investigate more plant indices and machine learning algorithms to increase models' accuracy and robustness. However, additional work is needed to consider how management and N impacts reflectance patterns can improve LAI prediction using UAV.

AUTHOR CONTRIBUTIONS

Joseph Sékou B. Dembele: Conceptualization; data curation; formal analysis; funding acquisition; methodology; software; writing—original draft. **Boubacar Gano:** Conceptualization; formal analysis; methodology; software; writing—review and editing. **Modou Mbaye:** Data curation; formal analysis; software. **Mohamed Doumbia:** Data curation; formal analysis. **LéonceLamine Dembele:** Data curation; formal analysis. **Mamoutou Kouressy:** Supervision. **Niaba Teme:** Writing—review and editing. **Michel Vaksman:** Conceptualization; methodology; writing—review and editing. **Diaga Diouf:** Supervision; writing—review and editing. **Alain Audebert:** Conceptualization; funding acquisition; methodology; project administration; supervision; writing—original draft.

ACKNOWLEDGMENTS

The authors are thankful to undergraduate all students, technicians, and workers of Sotuba agroclimatology unity that helped us in achievement this work. This research activity was also funded in part by Bill and Melinda Gates foundation under Sorghum Genotyping Tools project and benefit the facilities of the Centre d'Etude Régional pour l'Amélioration de l'Adaptation à la Sécheresse (CERAAS).

CONFLICT OF INTEREST STATEMENT

The authors declare no conflicts of interest.

ORCID

Joseph Sékou B. Dembele  <https://orcid.org/0000-0003-2889-7457>

REFERENCES

- Anguiby, B. L. A., Ouattara, G., Bomisso, E. L., N'goran, B., Ouattara, B., Coulibaly, S. A., & Aké, S. (2019). Effet de la date et de la densité de semis sur la croissance et le rendement en grain du mil tardif [*Pennisetum glaucum* (L.) R. Br] dans les zones sud est et sud du Sénégal. *Journal Applied Bioscience*, *138*, 14106–14122. <https://doi.org/10.4314/jab.v138i1.9>
- Carmer, S. G., Nyquist, W. E., & Walker, W. M. (1989). Least significant differences for combined analyses of experiments with two- or three-factor treatment designs. *Journal of Agronomy*, *81*, 665–672. <https://doi.org/10.2134/agronj1989.00021962008100040021x>
- CEDEAO-UEMOA-CILSS. (2016). *Catalogue Régional des Espèces et Variétés Végétales CEDEAO-UEMOA-CILSS*.
- Chapman, S., Merz, T., Chan, A., Jackway, P., Hrabar, S., Dreccer, M., Holland, E., Zheng, B., Ling, T., & Jimenez-Berni, J. (2014). Phenocopter: A low-altitude, autonomous remote-sensing robotic helicopter for high-throughput field-based phenotyping. *Agronomy*, *4*, 279–301. <https://doi.org/10.3390/agronomy4020279>
- Chawade, A., Armoniené, R., Berg, G., Brazauskas, G., Frostgård, G., Geleta, M., Gorash, A., Henriksson, T., Himanen, K., Ingver, A., Johansson, E., Jørgensen, L. N., Koppel, M., Koppel, R., Makela, P., Ortiz, R., Podyma, W., Roitsch, T., Ronis, A., ... Weih, M. (2018). A transnational and holistic breeding approach is needed for sustainable wheat production in the Baltic Sea region. *Physiology Plant*, *164*, 442–451. <https://doi.org/10.1111/ppl.12726>
- Chawade, A., Van Ham, J., Blomquist, H., Bagge, O., Alexandersson, E., & Ortiz, R. (2019). High-throughput field-phenotyping tools for plant breeding and precision agriculture. *Agronomy*, *9*, 258. <https://doi.org/10.3390/agronomy9050258>
- Cheng, Z., Meng, J., Shang, J., Liu, J., Huang, J., Qiao, Y., Qian, B., Jing, Q. I., Dong, T., & Yu, L. (2020). Generating time-series LAI estimates of maize using combined methods based on multispectral UAV observations and WOFOST modeling. *Sensors*, *20*, 6006. <https://doi.org/10.3390/s20216006>
- Dembele, J. S. B., Gano, B., Kouressy, M., Dembele, L. L., Doumbia, M., Ganyo, K. K., Sanogo, S., Togola, A., Traore, K., Vaksman, M., Teme, N., Diouf, D., & Audebert, A. (2021). Plant density and nitrogen fertilization optimization on sorghum grain yield in Mali. *Agronomy Journal*, *113*, 4705–4720. <https://doi.org/10.1002/agj.2.20850>
- Dembélé, J. S. B., Gano, B., Vaksman, M., Kouressy, M., Dembele, L. L., Doumbia, M., Teme, N., Diouf, D., & Audebert, A. (2020). Response of eight sorghum varieties to plant density and nitrogen fertilization in the Sudano-Sahelian zone in Mali. *African Journal of Agricultural Research*, *16*(10), 1401–1410. <https://doi.org/10.5897/AJAR2020.15025>
- Din, M., Zheng, W., Rashid, M., Wang, S., & Shi, Z. (2017). Evaluating hyperspectral vegetation indices for leaf area index estimation of *Oryza sativa* L. at diverse phenological stages. *Frontier Plant Science*, *8*, 820. <https://doi.org/10.3389/fpls.2017.00820>
- Fiorani, F., & Schurr, U. (2013). Future scenarios for plant phenotyping. *Annual Review of Plant Biology*, *64*, 267–291. <https://doi.org/10.1146/annurev-arplant-050312-120137>
- Gano, B., Dembele, J. S. B., Ndour, A., Luquet, D., Beurier, G., Diouf, D., & Audebert, A. (2021). Adaptation responses to early drought stress of West Africa sorghum varieties. *Agronomy*, *11*(5), 850. <https://doi.org/10.3390/agronomy11050850>
- Gano, B., Dembele, J. S. B., Ndour, A., Luquet, D., Beurier, G., Diouf, D., & Audebert, A. (2021). Using UAV borne, multi-spectral

- imaging for the field phenotyping of shoot biomass, leaf area index and height of West African sorghum varieties under two contrasted water conditions. *Agronomy*, 2021, 11, 850. <https://doi.org/10.3390/agronomy11050850>
- Gitelson, A. A., & Merzlyak, M. N. (1998). Remote estimation of chlorophyll content in higher plant leaves. *Advances in Space Research*, 22(5), 689–692. [https://doi.org/10.1016/S0273-1177\(97\)01133-2](https://doi.org/10.1016/S0273-1177(97)01133-2)
- Gondal, M., Hussain, A., Yasin, S., Musa, M., & Rehman, H. (2017). Effect of seed rate and row spacing on grain yield of sorghum. *SAARC Journal Agricultural*, 15(2), 81–91. <https://doi.org/10.3329/sja.v15i2.35154>
- Gong, Y., Yang, K., Lin, Z., Fang, S., Wu, X., Zhu, R., & Peng, Y. (2021). Remote estimation of leaf area index (LAI) with unmanned aerial vehicle (UAV) imaging for different rice cultivars throughout the entire growing season. *Plant Method*, 17(2021), 88. <https://doi.org/10.1186/s13007-021-00789-4>
- Gracia-Romero, A., Kefauver, S. C., Vergara-Díaz, O., Zaman-Allah, M. A., Prasanna, B. M., Cairns, J. E., & Arous, J. L. (2017). Comparative performance of ground vs. aerially assessed RGB and multispectral indices for early-growth evaluation of maize performance under phosphorus fertilization. *Frontier Plant Science*, 8, 2004. <https://doi.org/10.3389/fpls.2017.02004>
- Gracia-Romero, A., Vergara-Díaz, O., Thierfelder, C., Cairns, J., Kefauver, S., & Arous, J. (2018). Phenotyping conservation agriculture management effects on ground and aerial remote sensing assessments of maize hybrids performance in Zimbabwe. *Remote Sensing*, 10, 349. <https://doi.org/10.3390/rs10020349>
- Hassan, M., Yang, M., Rasheed, A., Jin, X., Xia, X., Xiao, Y., & He, Z. (2018). Time-series multispectral indices from unmanned aerial vehicle imagery reveal senescence rate in bread wheat. *Remote Sensing*, 10, 809. <https://doi.org/10.3390/rs10060809>
- Huang, J., Sedano, F., Huang, Y., Ma, H., Li, X., Liang, S., Tian, L., Zhang, X., Fan, J., & Wu, W. (2016). Assimilating a synthetic Kalman filter leaf area index series into the WOFOST model to improve regional winter wheat yield estimation. *Agriculture for Forest Meteorology*, 216, 188–202. <https://doi.org/10.1016/j.agrformet.2015.10.013>
- Jay, S., Baret, F., Dutartre, D., Malatesta, G., Héno, S., Comar, A., Weiss, M., & Maupas, F. (2019). Exploiting the centimeter resolution of UAV multispectral imagery to improve remote-sensing estimates of canopy structure and biochemistry in sugar beet crops. *Remote Sensing Environment*, 231, 110898. <https://doi.org/10.1016/j.rse.2018.09.011>
- Jin, X.-L., Diao, W.-Y., Xiao, C.-H., Wang, F.-Y., Chen, B., Wang, K.-R., & Li, S.-K. (2013). Estimation of wheat agronomic parameters using new spectral indices. *PLoS One*, 8, e72736. <https://doi.org/10.1371/journal.pone.0072736>
- Kang, Y., Özdoğan, M., Zipper, S., Román, M., Walker, J., Hong, S., Marshall, M., Magliulo, V., Moreno, J., Alonso, L., Miyata, A., Kimball, B., & Loheide, S. (2016). How universal is the relationship between remotely sensed vegetation indices and crop leaf area index? A global assessment. *Remote Sensing*, 8(7), 597. <https://doi.org/10.3390/rs8070597>
- Kouressy, M., Sissoko, S., Tékété, M. L., Sanogo, S., Kamissoko, S., Doumbia, M., Sissoko, A., Théra, K., Dingkhun, M., Koné, A. S., Ouattara, M., Vaksmann, M., & Témé, N. (2020). Sélection du sorgho pour une intensification durable au Mali. Apports de la modélisation des cultures. In B Sultan, A. Y. Bossa, S. Salack, & M. Sanon (Eds.), *Risques climatiques et agriculture en Afrique de l'Ouest variétés* (pp. 337–352). IRD Éditions.
- Leakey, A. D. B., Ainsworth, E. A., Bernacchi, C. J., Rogers, A., Long, S. P., & Ort, D. R. (2009). Elevated CO₂ effects on plant carbon, nitrogen, and water relations: Six important lessons from face. *Journal Experimental Botanic*, 60, 2859–2876. <https://doi.org/10.1093/jxb/erp096>
- Malambo, L., Popescu, S. C., Murray, S. C., Putman, E., Pugh, N. A., Horne, D. W., Richardson, G., Sheridan, R., Rooney, W. L., Avant, R., Vidrine, M., Mccutchen, B., Baltensperger, D., & Bishop, M. (2018). Multitemporal field-based plant height estimation using 3D point clouds generated from small unmanned aerial systems high-resolution imagery. *International Journal of Applied Earth Observation and Geoinformation*, 64, 31–42. <https://doi.org/10.1016/j.jag.2017.08.014>
- McIntyre, B. D., Herren, H. R., Wakhungu, J., & Watson, R. T. (2009). *Agriculture at a crossroads: Global report*. International Assessment of Agricultural Knowledge, Science and Technology for Development (IAASTD). Sub-Saharan Africa (SSA). <https://wedocs.unep.org/20.500.11822/8590>
- Melaku, N. D., Bayu, W., Ziadat, F., Strohmeier, S., Zucca, C., Tefera, M. L., Ayalew, B., & Klik, A. (2017). Effect of nitrogen fertilizer rate and timing on sorghum productivity in Ethiopian highland Vertisols. *Archives Agronomy Soil Science*, 64, 480–491. <https://doi.org/10.1080/03650340.2017.1362558>
- Naser, M., Khosla, R., Longchamps, L., & Dahal, S. (2020). Using NDVI to differentiate wheat genotypes productivity under dryland and irrigated conditions. *Remote Sensing*, 12, 824. <https://doi.org/10.3390/rs12050824>
- Peng, Y. I., Gitelson, A. A., Keydan, G., Rundquist, D. C., & Moses, W. (2011). Remote estimation of gross primary production in maize and support for a new paradigm based on total crop chlorophyll content. *Remote Sensing Environment*, 115, 978–989. <https://doi.org/10.1016/j.rse.2010.12.001>
- Potgieter, A. B., George-Jaeggli, B., Chapman, S. C., Laws, K., Suárez Cadavid, L. A., Wixted, J., Watson, J., Eldridge, M., Jordan, D. R., & Hammer, G. L. (2017). Multi-spectral imaging from an unmanned aerial vehicle enables the assessment of seasonal leaf area dynamics of sorghum breeding lines. *Frontier Plant Science*, 8, 1532. <https://doi.org/10.3389/fpls.2017.01532>
- Prasad, B., Carver, B. F., Stone, M. L., Babar, M. A., Raun, W. R., & Klatt, A. R. (2007). Potential use of spectral reflectance indices as a selection tool for grain yield in winter wheat under great plains conditions. *Crop Science*, 47, 1426–1440. <https://doi.org/10.2135/cropsci2006.07.0492>
- Raun, W. R., Solie, J. B., Johnson, G. V., Stone, M. L., Lukina, E. V., Thomason, W. E., & Schepers, J. S. (2001). In-season prediction of potential grain yield in winter wheat using canopy reflectance. *Agronomy Journal*, 93, 131–138. <https://doi.org/10.2134/agronj2001.931131x>
- Ray, D. K., Mueller, N. D., West, P. C., & Foley, J. A. (2013). Yield trends are insufficient to double global crop production by 2050. *PLoS One*, 8, e66428. <https://doi.org/10.1371/journal.pone.0066428>
- Roupsard, O., Audebert, A., Ndour, A. P., Clermont-Dauphin, C., Agbohossou, Y., Sanou, J., Koala, J., Faye, E., Sambakhe, D., Jourdan, C., Le Maire, G., Tall, L., Sanogo, D., Seghieri, J., Cournac, L., & Leroux, L. (2020). How far does the tree affect the crop in agroforestry? New spatial analysis methods in a *Faidherbia*

- parkland. *Agriculture, Ecosystems, and Environment*, 296(2020), 106928. <https://doi.org/10.1016/j.agee.2020.106928>
- Rouse, J. W., Hass, R. H., Schell, J. A., & Deering, D. W. (1973). Monitoring vegetation systems in the Great Plains with erts. In *Proceedings of the third Earth resources technology satellite symposium* (pp. 309–317). NASA.
- Serrano, L., Filella, I., & Peñuelas, J. (2000). Remote sensing of biomass and yield of winter wheat under different nitrogen supplies. *Crop Science*, 40, 723–731. <https://doi.org/10.2135/cropsci2000.403723x>
- Shafian, Z., Rajan, N., Ronnie Schnell, R., Bagavathiannan, M., Valasek, J., Shi, Y., & Olsenholler, J. (2018). Unmanned aerial systems-based remote sensing for monitoring sorghum growth and development. *PLoS One*, 13(5), e0196605. <https://doi.org/10.1371/journal.pone.0196605>
- Smale, M., Assima, A., Kergna, A., Thériault, V., & Weltzien, E. (2018). Farm family effects of adopting improved and hybrid sorghum seed in the Sudan Savanna of West Africa. *Food Policy*, 74(2018), 162–171. <https://doi.org/10.1016/j.foodpol.2018.01.001>
- Soudani, K., Trautmann, J., & Walter, J.-M. (2001). Comparaison de méthodes optiques pour estimer l'ouverture de la canopée et l'indice foliaire en forêt feuillue. *Comptes Rendus de l'Académie des Sciences—Séries III—Sciences de la vie*, 324(2001), 381–392. [https://doi.org/10.1016/S0764-4469\(00\)01294-4](https://doi.org/10.1016/S0764-4469(00)01294-4)
- Sultana, S. R., Ali, A., Ahmad, A., Mubeen, M., Zia-Ul-Haq, M., Ahmad, S., Ercisli, S., & Jaafar, H. Z. E. (2014). Normalized difference vegetation index as a tool for wheat yield estimation: A case study from Faisalabad, Pakistan. *Scientific World Journal*, 2014, 725326. <https://doi.org/10.1155/2014/725326>
- Towers, P. C., Strever, A., & Poblete-Echeverría, C. (2019). Comparison of vegetation indices for leaf area index estimation in vertical shoot positioned vine canopies with and without grenbiule hail-protection netting. *Remote Sensing*, 11, 1073. <https://doi.org/10.3390/rs11091073>
- Venables, W. N., Smith, D. M., & R Development Core Team. (2016). *An introduction to R: Notes on R, a programming environment for data analysis and graphics*. <https://onlinebooks.library.upenn.edu/webbin/book/lookupid?key=olbp44950>
- Wezel, A., Casagrande, M., Celette, F., Vian, J.-F., Ferrer, A., & Peigné, J. (2014). Agroecological practices for sustainable agriculture. A review. *Agronomy Sustainable Development*, 34, 1–20. <https://doi.org/10.1007/s13593-013-0180-7>
- Wilhelm, W. W., Ruwe, K., & Schlemmer, M. R. (2000). Comparison of three leaf area index meters in a corn canopy. *Crop Science*, 40, 1179–1183. <https://doi.org/10.2135/cropsci2000.4041179x>
- Yang, G., Liu, J., Zhao, C., Li, Z., Huang, Y., Yu, H., Xu, B., Yang, X., Zhu, D., Zhang, X., Zhang, R., Feng, H., Zhao, X., Li, Z., Li, H., & Yang, H. (2017). Unmanned aerial vehicle remote sensing for field-based crop phenotyping: Current status and perspectives. *Frontier Plant Science*, 8, 1111. <https://doi.org/10.3389/fpls.2017.01111>
- Yang, M., Hassan, M. A., Xu, K., Zheng, C., Rasheed, A., Zhang, Y., Jin, X., Xia, X., Xiao, Y., & He, Z. (2020). Assessment of water and nitrogen use efficiencies through UAV-based multispectral phenotyping in winter wheat. *Frontier Plant Science*, 11, 927. <https://doi.org/10.3389/fpls.2020.00927>

How to cite this article: Dembele, J. S. B., Gano, B., Mbaye, M., Doumbia, M., Dembele, L. L., Kouressy, M., Teme, N., Vaksman, M., Diouf, D., & Audebert, A. (2024). Unmanned aerial vehicle imagery prediction of sorghum leaf area index under water stress, seeding density, and nitrogen fertilization conditions in the Sahel. *Agronomy Journal*, 116, 1003–1014. <https://doi.org/10.1002/agj2.21547>